

Antigens from H22 cell mutation induced by lentinan are correlated with HCC immunoprophylaxis

Xin Yang

Hebei University of Science and Technology

Yandong Li

Laboratory of Veterinary Drug Residues, Hebei Institute of Veterinary Drugs Control

Wen Wang

Hebei University of Science and Technology

Chong Li

Hebei University of Science and Technology

Dandan Zhao

Hebei University of Science and Technology

Gaoshuang Hu

Hebei University of Science and Technology

Huan Rao

Hebei University of Science and Technology

Jianxiong Hao

Hebei University of Science and Technology

Xue Han (✉ hanxue_h@163.com)

Hebei University of Science and Technology

Research

Keywords: Immunogen, Immune prophylaxis, Liver cancer, Cellular immunity, Cytokines, Protein mass spectrometry

Posted Date: July 23rd, 2020

DOI: <https://doi.org/10.21203/rs.3.rs-43542/v1>

License:   This work is licensed under a Creative Commons Attribution 4.0 International License.

[Read Full License](#)

Abstract

Background Lentinan can inhibit the proliferation of many kinds of tumor cells, and some studies have shown that lentinan can inhibit the growth of tumor tissue by directly killing tumor cells. The purpose of this study was to investigate the immunoprophylaxis effect and mechanism of tumor specific antigen induced by lentinan on liver cancer in mice.

Methods The immunogen was prepared which was induced by lentinan. And two different mouse H22 liver cancer models (ascites tumor and solid tumor) were established after immunogen immunized. The tumor growth and immune organ index of mice in each group were measured. In order to analyze the immune mechanism, the activity of CTL cells, activation of ADCC pathway, T lymphocyte subsets, expression of CD4 + T, CD8 + T cells and expression of DC, and surface molecular markers CD80 and CD86 in immunized mice were analyzed. The expression of cytokines such as IFN- γ and TNF- α in serum and cell supernatant of mice in each group was tested too. Finally, the immunogen was analyzed by Liquid Chromatography-Mass Spectrometry (LC-MS), and the functional proteins were screened for further analysis.

Results The liver, spleen and thymus of the mice immunized with immunogen were protected to a certain extent. In immunized mice, the proportion of CD4 + T cells increased, the proportion of CD8 + T cells decreased, the ratio of CD4 + T/CD8 + T increased, and the killing activity of T lymphocytes increased significantly. The expression of CD80 in mature DC cells of immunized mice increased and cytokines increased significantly. The results of protein mass spectrometry analysis of immunogen showed that immunogen produced protein properties that inhibit cancer.

Conclusion The H22 whole-cell cleavage vaccine induced by lentinan is effective in the immunity of mouse hepatoma H22 and has development value in the future.

Background

Hepatocellular carcinoma is the third leading cause of cancer-related deaths in the world[1]. In recent years, the incidence of liver cancer in China has shown an upward trend, the case fatality rate has also increased, and the incidence of liver cancer is getting younger. If hepatitis B and C are not treated in time, they may turn into chronic hepatitis and eventually cirrhosis[2]. There is an inevitable link between liver cancer and liver cirrhosis. Studies have shown that most of patients with liver cirrhosis are transformed into liver cancer due to untimely treatment. The main factors inducing primary liver cancer are hepatitis virus, aflatoxin B, tobacco, vinyl chloride, alcohol intake, non-alcoholic fatty liver disease and diabetes. Because the diagnosis of HCC is usually in the middle and advanced stage, the best treatment time has been missed, and the current conventional treatment can not be cured. Tumor resection, chemotherapy, radiotherapy, various embolization and sorafenib have been used in the clinical treatment of liver cancer[3]. However, the recurrence rate after surgical resection is very high, and the 5-year survival rate after operation is only 18%[4], so immune replacement therapy shows the necessity for the treatment

of liver cancer. Three different kinds of hepatocytes, namely sinusoidal endothelial cells(LSEC)[5], Kupffer cells[6] and dendritic cells (DC), are mainly involved in the immune response of HCC patients. The emergence of effector T cells after surgical transplantation reduces the risk of recurrence, which is the key to antibody therapy. The combination of monoclonal antibody (mAbs) or chemotherapy and transarterial chemoembolization are the main methods to improve the overall survival rate of HCC patients[7]. Tumor associated antigen (TAA) is a non-specific antigen, and its expression imbalance leads to immune response deficiency. CD8 + T cells have the potential to reverse tumor inhibitory microenvironment[8]. The antigenicity of tumor associated antigens comes from somatic gene mutations, resulting in abnormal regulation of carcinoembryonic proteins and testicular antigens. Although targeted immune molecules can inhibit T cell activation, but cytotoxic T lymphocyte antigen-4 (CTLA-4), the expression of programmed cell death protein 1 (PD-1), PD ligand (PD-L1) was not affected. Anti-GPC3 also showed good efficacy in phase II clinical trials of patients with advanced HCC.

The anti-tumor immune mechanism of the body is very complex, involving a variety of immune cells and the products secreted by them. It can be divided into cellular immunity and humoral immunity as well as cytokines[9]. Cellular immunity is mainly mediated by T lymphocytes, NK cells and macrophages, and has anti-tumor effect. Recent studies have shown that activated immune cells secrete cytokines can play a direct role in anti-tumor by immunomodulatory effect[10]. Immune cells interact with antibodies to enhance the anti-tumor mechanism. At present, most scholars believe that the lentinan can inhibit the proliferation of many kinds of tumor cells, and lentinan may inhibit the growth of tumor tissue by directly killing tumor cells[11]. The immunogenicity of tumor cells will be enhanced with the apoptosis induced by lentinan. In order to solve the problem of immune prevention of liver cancer and test the effect of immunogen induced by lentinan, H22 liver cancer cells ascites tumor and solid tumor models were set up, and lentinan was used as inducer to prepare immunogen. To explore the immune preventive mechanism of tumor specific antigen induced by lentinan on HCC in mice, it will play an important role in the development and application of prophylactic liver cancer vaccine in the future.

Materials And Methods

Lab mice

SPF female KM mice weighed 18-22g were purchased from the animal center of Hebei Medical University (SCXK (JI)2013-1-003, 1410014, Shijiazhuang, China). The mice were maintained in an environment with controlled temperature (20 to 25°C) and humidity (50% ± 5%), with food and water available at any time and a natural light. The health of the mice was monitored every day. Before blood collection or immune organ index test, mice were anesthetized with ether, and the other mice were euthanized by cervical dislocation under anesthesia with isoflurane.

Cell lines and lentinan

The murine liver cancer cell line H22 cells (China PLA General Hospital, Beijing, China) were cultured in RPMI 1640 medium supplemented with 10% heat-inactivated fetal bovine serum (FBS) and antibiotics

(100 u/mL penicillin and 100 g/mL streptomycin) at 37°C in an atmosphere of 5% CO₂[12]. Lentinan used in this study was gifted from Kang Yuan (Jiangsu, China).

Immunogen preparation

We need to co-culture cancer cells with lentinan. H22 cells suspension (1×10^7) and lentinan solution (170µL/mg). The co-cultures were cultured at 37 °C and 5% CO₂ for 48 hours. The co-cultures were frozen and thawed repeatedly in a low temperature refrigerator of -80 °C, then centrifuged and purified for immune test. Finally, the concentration of antigen protein was determined by Coomassie brilliant blue method[13].

Immunization protocol

A sample of 100 mice were randomly and equally divided into 5 groups, including divided equally among the control group, model-1 group, model-2 group, LHA-1 group and LHA-2 group(n = 20). The LHA-1 group and LHA-2 group were treated intraperitoneally (i.p.) with antigens (0.2 mL/mouse), once per week for 3 weeks. The mice in control and model groups were treated with 0.9% normal saline. One week after the third immunization, all of the mice except the control group were inoculated with H22 cells (1.5×10^6 cells/mouse). The model-1 group and LHA-1 group were inoculated with H22 cells with i.p to establish the H22 ascitic tumor model[14]. And the model-2 group and LHA-2 group were inoculated with H22 cells with s.c(subcutaneous) to establish the H22 solid tumor model[15]. From day 10 to day 21, the tumor size of tumor bearing mouse was tested by vernier calip. 21 days after establishment of the H22 mouse models, the body weights of the mice in each group were recorded.

Tumor incidence and immune organ index

Ten mice in each group were selected randomly to calculate the volume and weight of the tumor, immune organ (thymus and spleen) index and cellular immunity. The spleen and thymus were collected from each mouse, and the growth index for each thymus or spleen was recorded[16].

$$\text{Spleen index} = \frac{\text{spleen weights(mg)}}{\text{body weights(g)}}$$

$$\text{Thymus index} = \frac{\text{thymus weights(mg)}}{\text{body weights(g)}}$$

HE staining

At the conclusion of the experiments, the tumors were harvested and stained with hematoxylin-eosin(HE) to discern the histopathological response and evaluate the tumors' morphology. HE staining was

conducted according to routine protocols[17]. Briefly, after deparaffinization and rehydration, 5 μm longitudinal sections were stained with hematoxylin solution for 5 min followed by 5 dips in 1% acid ethanol (1% HCl in 70% ethanol) and then rinsed in distilled water. Then the sections were stained with eosin solution for 3 min and followed by dehydration with graded alcohol and clearing in xylene. The mounted slides were then examined and photographed using an Olympus BX53 fluorescence microscope (Tokyo, Japan).

Scanning electron microscopy

For studies, solid tumors were cut and the size of the tissue block was 1 mm³. The specimens were cleaned with normal saline and then were fixed with 4% paraformaldehyde at 4°C for 3 hours, 10~15min per time. After drying with alcohol gradient dehydration (50%, 70%, 80%, 90%, 100%) for two times, and 75% and 100% tert-butanol on 4°C for 10 min orderly, the specimens were gold coated by sputtering (SCD 040 Balzers device, Bal-Tec)[18]. The samples were then examined with a Cambridge Stereoscan 360 scanning electron microscope (Cambridge Instruments, Cambridge, United Kingdom).

Splenocyte lymphocyte proliferation experiment

The mice were sacrificed and the spleens were obtained, and then the spleen cell suspension was obtained after washing, grinding and centrifugal lysis. The T lymphocyte transformation test and B lymphocyte transformation experiment were carried out according to the instructions of the kit(American Biologend Co., Ltd.). With the results were tested at 570nm, the stimulation index was calculated to judge the proliferation rate of T lymphocytes and B lymphocytes[19]. The stimulation index is according to the following formula.

CTL cell killing activity detection

The immunized mouse spleen cells (effector cells) suspension was taken, and the cell concentration was adjusted to 1×10⁵cells/mL, by adding 10% fetal bovine serum medium RPMI-1640. The spleen cells suspension was cultured at 37°C for 24 hours. According to the ratio of 50: 1(spleen cells: H22 cells), H22 cells(target cells) were added into spleen cells suspension for coculture. Three multiple samples were set up in each group and cultured for 24 hours. After that, MTT solution (5g/L) 20μL was added to each well and cultured at 37 °C for 4 hours before centrifugation. Dimethyl sulfoxide (DMSO) was added to each well and placed for 20 minutes after shaking. The absorbance under 490nm was measured by enzyme labeling instrument, and then the cytotoxicity of CTL cells was calculated by the following formula.

$$CTL \text{ cellkilling activity} = \frac{[1 - (OD \text{ effect} - \text{target cell} - OD \text{ effector cell})]}{OD \text{ target cell}} \times 100\%$$

Analysis of antibody-dependent cell-mediated cytotoxicity (ADCC pathway)

Splenocytes were prepared following the method described previously (Xu et al., 2019). The immune antiserum was diluted 1:50 times with complete RPMI 1640 medium. To confirm the role of antigen in ADCC activation induced by lentinan, H22 cells were seeded into a 96-well microplate at 1×10^5 cells/well in a complete RPMI 1640 medium and treated without (control) or with Spleen lymphocytes and antiserum (LA), Spleen lymphocytes (SL) and antiserum (AS) respectively, and then were subjected to MTT method. The absorbance in each well was determined at 570 nm by using a microplate reader (Multiskan FC, Thermo, USA). The following formula was used for calculating the proliferation ratio:

$$pr = \frac{A_{570 \text{ of experimental group}}}{A_{570 \text{ of control group}}} \times 100\%$$

Flow cytometry was used to determine CD4+T and CD8+T in T cell subsets

Splenic lymphocyte were aseptically isolated from KM mice. After carefully removed, the spleens were minced in HBSS and filtered through a 200-mesh sterile strainer. The pelleted cells were obtained by centrifugation at 1000 rpm for 5 min. Subsequently, lymphocyte separation medium was employed to enrich the lymphocytes, followed by resuspension in a complete RPMI 1640 medium (1640 medium supplemented with 100 UI/ml penicillin, 100 µg/ml streptomycin and 10% heat inactivated FBS) and adjustment to 1×10^7 cells/ml with a haemocytometer by trypan blue dye exclusion assay. Lymphocytes were collected and stained using FITC anti-mouse CD4 +T antibody (Biolegend) and PE anti-mouse CD8 +T antibody (Biolegend). Then the cells were washed twice with PBS and subjected to FCM (BD Biosciences, San Jose, California, USA) analysis.

CD80 and CD86 subsets of DC cells were analyzed by flow cytometry

Murine bone marrow cells derived from femurs and tibiae were collected and suspended with Tris-NH₄Cl solution for 2 ~ 4 minutes at room temperature to lyse erythrocytes. After washed with PBS solution for twice, the bone marrow cells were cultured for 7 days at a density of 1×10^6 cells/ml in RPMI medium (Thermo, USA) supplemented with 10% FBS (Gibco, Carlsbad, California, USA), 10 units/ml penicillin, 10 µg/ml streptomycin, 2 mM L-glutamine (Gibco, USA) (hereafter termed complete medium) and 25 ng/ml murine GM-CSF (Miltenyi Biotech, Germany) at 37°C in a humidified atmosphere with 5% CO₂. On day 3, floating cells were discarded and fresh medium containing 25 ng/ml GM-CSF was added. Cells were further differentiated for 4 days with GM-CSF containing complete RPMI 1640 medium. Floating Lymphocytes were collected and stained using FITC anti-mouse CD11c antibody (Biolegend), PE-Cy5 anti-mouse CD80 antibody (Biolegend), and PE anti-mouse CD86 antibody (Biolegend). Then the cells were washed twice with PBS and subjected to FCM analysis.

Analysis of cytokine expression

The lymphocyte suspension was taken and the concentration was adjusted to 2×10^6 cells/mL. The prepared H22 cell suspension was added to the 96-well plate, and 100ul was added to each well. In the experimental group, 100ul splenocyte suspension was added to each well, and 3 repetitive wells were set

up. The control group did not add H22 cell suspension, and then the 96-well plate was cultured in a carbon dioxide incubator at 5% CO₂ and 37 degrees Celsius for 24 hours. After collecting the supernatant of cells, IFN- γ and TNF- α in serum and splenocytes were determined by ELISA kit.

Analysis of antigen by Liquid Chromatography-Mass Spectrometry (LC-MS)

The protein sample of antigens was further concentrated using Amicon Ultra-15 centrifugal filter MWCO3000 (Millipore) and measured by Bradford Assay (Solarbio, Bradford Protein Assay Kit, Beijing, China). An aliquot of the concentrated preparation containing 100 μ g protein was diluted with 50 mM NH₄HCO₃ to 70 μ L and added DTT with final concentration 10mM at 56°C for 1 h. The sample was then incubated with iodoacetamide (10mM final concentration) at room temperature for 40 minutes before digestion with trypsin (trypsin:protein 1:50 w/w) at 37 °C for 14 h. After speed-vac, the sample peptides were reconstituted in 50 mM NH₄HCO₃ for LC-MS analysis. LC/MS was performed on Thermo Scientific™ Q Exactive equipped with a Nanospray Floex Ion-Source. Peptides suspension dissolved in 0.1% formic acid were separated by nano- high performance liquid chromatography (Eksigent Technologies) on a secondary reversed-phase analytical column (Eksigent, C18, 3 μ m, 150 mm * 75 μ m). Buffer A for the pump consisted of 0.1% formic acid in LC/MS-grade water. Buffer B for the pump consisted of 0.1% formic acid in LC/MS-grade acetonitrile. Gradient conditions for pump B were as follows: 0% to 35% B from 0 to 90 minutes. A total of 5 mL of the prepared peptides was injected onto the trap column for concentration/purification. Flow rates were 300 nL/min. Some parameters in Orbitrap were as follows: spray voltage, 2.0 kV; capillary temperature, 250°C; m/z (mass to charge ratio) range (ms), 350 to 1800. AGC ion injection targets for each FTMS scan were 70,000 (100 ms max injection time). AGC ion injection targets for each MS2 scan were 17,500 (50 ms max ion injection time). Full MS/dd-MS2 (Top10) was used in this analysis, with a dynamic exclusion time of 25 s. Both identification and quantification were done by Proteome Discoverer (version 2.1 demo, Thermo Fischer Scientific). Uniprot-mouse database was used for data mining. Peptides were generated from a tryptic digestion with up to 2 missed cleavages, dynamic modifications of methionine oxidation, and a static modification of cysteine carbamidomethylation. Precursor mass tolerance was 10 ppm, and product ions were searched at 0.02-Da tolerances. Peptide spectral matches were validated using percolator based on q-values at a 1% false discovery rate.

Statistical processing

The data were analyzed using SPSS software (version 11.5, SPSS, New York, NY, USA) and $P < 0.05$ was considered as statistically significant. All the data were presented as mean \pm SD.

Results

Changes of body weight and tumor tissue in mice

From the day of modeling, the body weights of ascites tumor and solid tumor mice were weighed and recorded every day. As shown in figure 1-a, there were differences in body weight among groups. The body weight of mice in the model-1 group increased rapidly after the fifth day. There was no significant change in body weight between LHA-1 group and control group. On the tenth day, the average body weight of mice in control group, model-1 group and LHA-1 group was 35.07g, 42.50g, 33.79g, respectively. On the 18th day, the mice were dissected and the tumor was weighed. As shown in figure 1-b, there were significant changes on the seventh day, and the body weight of mice in the model-1 group increased rapidly and showed an upward trend all the time. On the 16th day, the average body weight of mice in control group, model-2 group and LHA-2 group was 35.58g, 43.78g and 35.39g, respectively. There was no significant change in body weight between control group and LHA-1 group. As shown in figure 1-c, solid tumors were clearly found in the armpits of mice in the model-2 group on the 10th day. Measured with Vernier caliper, the average volume of axillary solid tumor in the LHA-2 group was 717.89mm³(Fig. 1d). The average volume of the axillary solid tumor in the LHA-2 group was 59.44mm³. On the 16th day, the solid tumor in the model-2 group increased to 3042.92mm³ and the solid tumor in the LHA-2 group was 238.96mm³. The mice were dissected on the 18th day and the solid tumor weight of each group was weighed. The mass of solid tumor in LHA-2 group(0.25g) was significantly lower than that in model-2 group(4.80g) .

Mouse immune organ index

The organ index is the primary observation index to judge the ability of the body[20]. The thymus index, spleen index, cardiac index, renal index, lung index and liver index of each group were obtained, as shown in the figure 2. The thymus index and spleen index of LHA-1 group were significantly different from those of model-1 group and control group (figure 2-a). There was no significant difference in cardiac index, renal index and lung index between the LHA-1 group and the model-1 group. In solid tumor mice, the spleen of LHA-2 group was significantly enlarged compared with control group, as shown in the figure 2-b . There was significant difference in thymus index between LHA-2 group and model-2 group ($P < 0.05$). This part of the results showed that the thymus and spleen of mice were protected by LHA.

HE staining results

The liver histomorphology of the LHA-2 group was orderly which hepatocytes were arranged radially and neatly (fig. 3). While in model-2 group, hepatocytes were arranged disorderly, central vein congestion, hepatocyte mass and blisters were produced. In control group, the structure of spleen cells was clear, and the arrangement of lymphocytes was tight, and there was no obvious division and differentiation. In model-2 group, the arrangement of spleen lymphocytes was relatively sparse, the number was relatively small, and there were obvious inflammatory factors invading. There was no significant difference between LHA-2 group and control group. In the control group, some cells in the thymic cortex were dense, neatly arranged and well-defined. In model-2 group, the tissue structure of thymus changed, the cortex became thinner, the structure was loose, a large number of thymocytes were apoptotic, and the thymocytes were arranged in vacuoles. Thymocytes in LHA-2 group were closely arranged, the same size,

round and plump, but compared with model-2 group, the difference was significant. In model-2 group, H22 hepatoma cells grew well, less necrotic cells, less stroma and compact arrangement of cells. A large area of cell necrosis could be observed in the LHA-2 group, and the number of cells in the cancer tissue was less than that in the model-2 group. The cells were loosely arranged, wrapped by fibrous tissue, and the tumor cells were mainly polygonal of different sizes, and the connective tissue was obvious.

Sem results of solid tumor

As can be seen from figure 4, in the view of 3.0Kv7.0nm × 6.00k, the surface of cells in model-2 group was uneven, with ridged protuberances, capillaries clearly visible, and flagella protruding on the edge. In LHA-2 group, the surface was uneven, with ridged protuberances, no obvious capillaries and flagellar tissue, disorganized. The experimental results showed that the capillaries in the tumor decreased significantly.

Lymphocyte proliferation of spleen cells

Lymphocyte proliferation test, also known as lymphoid transformation test, is a basic technique for the detection of cellular immunological function. According to figure 5-a, the B cell and T cell stimulation index of model-1 group was 1.64 and 1.79 respectively. The B cell and T cell stimulation index of LHA-1 group were improved by 4.75 and 4.77 respectively, and the B cell stimulation index of model-1 group was significantly higher than that of LHA-1 group ($P < 0.05$). The results showed that LHA could significantly improve the immune level of B cells and T cells in tumor-bearing mice.

The detection of cytotoxic activity of CTL cells

As shown in figure 5-b, the CTL cell killing rate was 75.29% in the control group and 35.64% in the model-1 group. Compared with the model-1 group, the killing rate in the LHA-1 group was significantly increased to 78.65%. And compared with the control group, there is no obvious change. The cytotoxic activity of CTL cells was significantly increased in mice immunized with LHA ($p < 0.05$).

Cytotoxicity mediated by antibody-dependent cells

ADCC is an antibody-dependent cell-mediated cytotoxic effect. As can be seen from figure 5-c, the serum of mice which was successfully immunized had an inhibitory effect on H22, but the effect was not significant, while H22 hepatocellular carcinoma cells were associated with serum and spleen of immunized mice. The co-culture of H22 cells significantly inhibited the proliferation of H22 cells. The blank control rat serum showed no inhibitory effect. The results showed that the antiserum, H22 cells and spleen cells could be effectively inhibited Cell proliferation.

The CD4 and CD8 phenotypes of T cells were detected by flow cytometry

Compared with control group, the percentage of CD4+T cells in model-1 group (20.07) decreased significantly, while the percentage of CD8+T cells increased significantly ($p < 0.05$). Compared with model-

1 group, the CD4+T value and CD4+T/CD8+T value of LHA-1 group increased significantly, while the percentage of CD8+T cells decreased significantly ($p<0.05$). It is suggested that the successful mice immunized with LHA can increase the expression rate of CD4+T lymphocytes and inhibit the expression of CD8+T lymphocytes, thus increasing the ratio of CD4+T/CD8+T and enhancing the killing activity of T lymphocytes[21], thus improving the immune mechanism of T lymphocytes and reducing the incidence of liver cancer.(Fig. 6a)

CD80 and CD86 phenotypes of DC cells were detected by flow cytometry

Flow cytometry used double staining of CD11c, CD86 and CD80 as specific antibodies of DC. The expression of CD11c in each component was higher than that of 80% CD11c. CD80 and CD86 was the specific marker molecule on the surface of mature DCs cells. The more CD86 and CD80 expression, the more mature DCs[22]. As can be seen from figure 6-b, the positive expression rates of CD80 in control group, model-1 group and LHA-1 group were 29.3%, 21.5%, 34.1%, 26.8%, 15.5% and 17.0%, respectively. The results showed that the expression of CD80 protein in DCs was increased by immunizing mice with LHA, thus promoting the maturation of DC. DC initiates the anti-tumor immune response by overexpressing the costimulatory molecule CD80 to provide the second signal necessary for T lymphocyte activation.

Results of cytokine expression

The concentrations of IFN- γ in serum were 121.60 pg/mL and 138.27 pg/mL and 181.60 pg/mL, respectively. There was significant difference between LHA-1 group and model-1 group ($p<0.05$). The expression level of IFN- γ in LHA-1 group was significantly higher than that in control group. The concentration of IFN- γ in the supernatant of control group, model-1 group and LHA-1 group was 2061.60 pg/mL and 2181.60 pg/mL and 5381.60 pg/mL, respectively. The expression level of IFN- γ in LHA-1 was significantly higher than that in control group and model-1 group. As shown in figure 4-3, there was no significant difference in the expression of TNF- α in serum among control group, model-1 group and LHA-1 group. The concentration of TNF- α in the supernatant of control group, model-1 group and LHA-1 group was 593.48pg/mL, 658pg/mL and 1545.1pg/mL. LHA-1 group was significantly different from that in model-1 group ($P<0.05$). The expression of TNF- α in model-1 group was lower than that in control group. The expression of TNF- α in LHA-1 immunization group was increased, and the expression level of TNF- α was significantly higher than that in model-1 group.(Fig. 6c, d)

Analysis of antigen by mass spectrometry

Among all the 310 antigenic proteins containing specific peptides, there were 32 new proteins. The molecular weight of tumor antigen induced by lentinan was similar to that of 47~60KDa[23]. By comparing with the database information in UniPort, 6 of the 32 new proteins were found to have anti-tumor effect. The main functions are summarized as follows: (1) The release can lead to tumor necrosis factor-related apoptosis-inducing ligand and induce cancer cell death. (2) It can inhibit the tumor by inhibiting the angiogenesis in the tumor tissue. (3) Directly inhibit the formation of invasion and

metastasis of cancer cells. Through the search and analysis of UniPort database, the following results are obtained:

Table 1 Analysis of new tumor suppressor proteins

N	Relative molecular weight(kDa)	Code	Protein name
1	47.965	P14211	Calreticulin
2	50.617	E9Q1G8	Septin-7
3	52.351	P46938	Transcriptional coactivator
4		D3YZP9	Coiled-coil domain-containing protein 6
	52.906		
5	59.2	Q8BKX1	Brain-specific angiogenesis inhibitor 1-associated protein 2
6	61.212	Q60598	Src substrate cortactin

Discussion

At present, most scholars believe that the anti-tumor effect of polysaccharides is due to its immunomodulatory effect in the body. Related experiments show that lentinan can inhibit the proliferation of many kinds of tumor cells, and lentinan may inhibit the growth of tumor tissue by directly killing tumor cells[11].

Lentinan can down-regulate Bcl-2 protein and up-regulate Bax, caspase-3, p53 protein to stimulate cell apoptosis[24]. By regulating Bcl-2 family-related proteins to act on mitochondria, caspase family proteins are activated. The interaction of cytokines eventually leads to cell DNA breakage, cell fragmentation and cell apoptosis[25]. Lentinan can inhibit the expression of cyclinB1 in the process of cyclin detection, hinder the cell cycle, force the cell not to continue to divide, and stay in the G2/M phase. At the same time, after mitosis is blocked, tumor cells will inevitably initiate programmed death. In the experiment, the recovery of H22 cells is critical, if the frozen cells can not quickly pass from -60 ~ -10 degrees Celsius, the cells will be damaged to varying degrees because of the ice crystals formed during this period of time. APC plays a key role in the anti-tumor function of immune response. Dendritic cell (DC) is the most effective APC and is closely related to HCC. Many studies have shown that DCs from peripheral blood and lymph nodes of patients with liver cancer is reduced, with immature phenotypes and impaired function. One study showed that the more DC detected in HCC nodules, the better the prognosis. The infiltration of DC in HCC nodules is closely related to the prognosis of patients with HCC after surgical resection [26]. The abnormal composition of DC in the hepatic lymph nodes of HCC patients may be one of the reasons for the insufficient response to HCC T cells in these patients[27]. In addition, some tumor-derived factors, such as vascular endothelial growth factor, granulocyte-macrophage colony-stimulating factor, IL-6 and IL-10, affect the differentiation, quantity and phenotype of DC. In view of the importance

of cancer development, DC is increasingly used to vaccinate a variety of cancers, including HCC. DC-based vaccines have been reported not only to induce tumor antigen-specific CTL, but also to activate NK cells and inhibit regulatory T cells in HCC patients. However, tumor tissue is not always available. Therefore, many researchers usually use peptides or cell line lysates to replace tumor tissue. At least in HCC, this alternative strategy has been proved to be feasible and secure. Tumor immunity produces cellular and humoral immunity through the recognition of tumor antigens by the immune system. Among them, cellular immunity plays a leading role, and humoral immunity and cellular immunity play an anti-tumor role[28]. At present, tumor immune cell therapy is mainly cytokine-induced lymphokine-activated killer cells, natural killer cells and more specific tumor infiltrating cells. They have direct killing effect on tumor cells and can present tumor specific antigens. Therefore, by measuring the proliferation of spleen cells, CTL cell killing activity and other related indicators, we can make a clear analysis of the anti-tumor immune mechanism of LHA[29]. Cytokines are low molecular weight peptides or proteins that can affect cell function and adapt it to cell-to-cell interactions. They are usually produced by cells with regulatory properties. Related studies have found that they will gather near the target cells or directly contact the target cells, and affect cell proliferation, differentiation and cell function by binding specific cell surface receptors[30]. The effects of cytokines on hematopoiesis and immune process include acute phase response and anti-tumor defense. By affecting the proliferation and diffusion of immune cells, differentiation, variation and physiological function to enhance the body's cellular and humoral immune response[31, 32]. Therefore, in this experiment, two significant representative factors in mouse serum and cell supernatant were determined.

From the point of view of antigen-specific peptides, we found several new proteins. Calreticulin (calreticulin, CRT) is a kind of Ca^{2+} binding protein with relative molecular weight of 46KD and highly conserved structure and function. It is mainly located in the endoplasmic reticulum and is also distributed in the nucleus and cell membrane. CRT has a variety of biological functions, such as molecular chaperone, regulation of Ca^{2+} homeostasis, cell adhesion, regulation of gene expression and so on. The treatment of U251 glioma with recombinant adenovirus vector containing SEPT7 can effectively up-regulate the expression of SEPT7, inhibit the activity of related members of matrix metalloproteinase (MMPs) family and up-regulate the expression of TIMP1/2. So as to inhibit the growth of tumor and reduce the ability of tumor invasion. It can be seen that SEPT7 can reverse the malignant phenotype of glioma cells, and SEPT7 can be further identified as a candidate tumor suppressor gene[33]. Brain-specific angiogenesis inhibitor 1 cooperates with ENAH to promote filipodia formation. It can inhibit tumor by inhibiting the formation of blood vessels in tumor tissue. In 1961, Folkman proposed that "the growth of tumors must depend on blood vessels", which was gradually accepted by people. Since then, the inhibition of angiogenesis has been the focus of anti-tumor therapy research. In recent years, some researchers have found that tumor blood vessels are the morphological basis of tumor cell growth and metastasis. tumor blood vessels not only provide nutrition to tumor cells, but also continuously transport tumor cells to other parts of the human body. leading to the growth and metastasis of malignant tumors [34]. Therefore, the inhibition of angiogenesis is an effective means to inhibit the growth and metastasis of tumor cells. A large number of literatures have reported that transcriptional coactivator (YAP1) has the

role of tumor suppressor genes in a variety of tumors, its expression is low in head and neck tumor cell lines and tumor tissues, and plays a role as a tumor suppressor gene[35].The low expression of YAP1 is highly correlated with many biological phenomena, such as the low expression of Akt, the phosphorylation of YAP1 in the nucleus, and the up-regulation of Δ NP63 and p73.YAP1 serine-127A alanine (S127A) mutation or knockout of Δ NP63 can enhance the nuclear localization and cell death of YAP1.On the contrary, knockout of YAP1 can increase cell proliferation, survival and migration, and resist the killing effect of cisplatin on tumor cells.Hippo-YAP1 interacts with other signal pathways to promote apoptosis or proliferation, and the specific mechanism and mode of action depend on the type of tissue or tumor.In addition, the subcellular localization of YAP1 also determines its functional characteristics. With the elucidation of a large number of signal pathways involved in YAP1 in recent years, YAP1 is expected to provide a new target for the treatment of some tumors[36].Glucocorticoid is a kind of important stress response hormone. Some experimental results show that the level of glucocorticoid in the body of people who have been in the state of chronic stress response for a long time continues to increase. Continuous stimulation of glucocorticoids can directly affect the biological behavior of tumors and play a role in inhibiting the formation of cancer cell invasion and metastasis[37].

Conclusions

In this study, lentinan was used as immune adjuvant to prepare liver cancer vaccine (LHA). Tumor specific antigen immune prevention induced by lentinan was studied from tumor growth, immune organs, immune cells, immune cytokines and protein regulation by zoology, immunology and bioinformatics. The results showed that the vaccine could inhibit the proliferation of H22 hepatoma cells and had immune effect on both solid tumor and ascites tumor. The cytotoxicity of T lymphocytes in immunized mice was enhanced, and DC promoted the maturation of CD8 through the high expression of costimulatory molecule CD80. Cytokines are also stimulated to express at a high level. Six new proteins can inhibit the production of tumor. The final result is that the H22 whole-cell cleavage vaccine induced by lentinan is effective in the immunity of mouse hepatoma H22 and has development value in the future.

Abbreviations

HCC:Hepatocellular carcinoma cancer;CTL:Cytotoxic T lymphocyte;LHA:Antigen induced by lentinan;CD:Clusters of differentiation;ADCC:Antibody-dependent cell-mediated cytotoxicity; DC:Dendritic cell;LC-MS:Liquid Chromatography-Mass Spectrometry;TAA:Tumor-associated antigen;NK:Natural killer cell;RPMI-1640:Roswell park memorial institute 1640;FBS:Fetal bovine serum;HE: Hematoxylin-eosin;MTT:Methylthiazolyldiphenyl-tetrazolium bromide;HBSS:Hank's balanced salt solution;FCM:Flow cytometry;ELISA:Enzyme linked immunosorbent assay;PMSF:Phenylmethylsulfonyl fluoride;DMSO:Dimethylsulfoxide.

Declarations

Competing interests

The authors declare that they have no competing interests.

Availability of data and materials

Data and material are available upon request.

Consent for publication

Not applicable.

Ethics approval and consent to participate

The study has been approved by the institutional ethical committee and all patients have signed the informed consent.

Ethics approval and consent to participate

All experiments were conducted following the Guide for the Care and Use of Laboratory Animals of National Institutes of Health. This study was approved by the animal ethics committee of Hebei University of Science and Technology.

Funding

Supported by Educational Commission of Hebei Province of China (ZD2019016) and Hebei Province Science Foundation for Youths (C2014208064).

Authors' contributions

X-Y, Y-DL and W-W participated in the collection and assembly of data, data analysis and interpretation, and manuscript writing. C-L and D-DZ participated in acquisition, analysis, and interpretation of data. G-SH, participated in the collection and assembly of the data and review of the manuscript. H-R participated in the design and supervision of research. J-XH and X-H conceived of the study, performed the statistical analysis, and helped to draft the manuscript. All authors read and approved the final manuscript.

Acknowledgements

Not applicable.

References

1. Lou LL, Zhang Y, Huang X, Zhang LX, Ji HF, Li X, Guo XL. Solitary nasopharynx metastasis from hepatocellular carcinoma after liver transplantation: A case report. *Med (Baltim)*. 2019;98(7):e14368.
2. Wang X, Li MM, Niu Y, Zhang X, Yin JB, Zhao CJ, Wang RT. Serum Zonulin in HBV-Associated Chronic Hepatitis, Liver Cirrhosis, and Hepatocellular Carcinoma. *Dis Markers*. 2019;2019:5945721.

3. Mazzanti R, Arena U, Tassi R. Hepatocellular carcinoma: Where are we? *World J Exp Med.* 2016;6(1):21–36.
4. Wang XH, Long LH, Cui Y, Jia AY, Zhu XG, Wang HZ, Wang Z, Zhan CM, Wang ZH, Wang WH. MRI-based radiomics model for preoperative prediction of 5-year survival in patients with hepatocellular carcinoma. *Br J Cancer.* 2020;122(7):978–85.
5. Thomas H. LSEC stretch promotes fibrosis during hepatic vascular congestion. *Nat Rev Gastroenterol Hepatol.* 2019;16(5):262–3.
6. Cheng Y, Chen T, Ping J, Chen J. Cangju Qinggan Jiangzhi Decoction Reduces the Development of NonAlcoholic Steatohepatitis and Activation of Kupffer Cells. *Cell Physiol Biochem.* 2018;48(3):971–82.
7. Vogl TJ, Oppermann E, Qian J, Imlau U, Tran A, Hamidavi Y, Korkusuz H, Bechstein WO, Nour-Eldin NE, Gruber-Rouh T, et al. Transarterial chemoembolization of hepatocellular carcinoma in a rat model: the effect of additional injection of survivin siRNA to the treatment protocol. *BMC Cancer.* 2016;16:325.
8. Li X, Lan X, Wang G, Liu Y, Zhao K, Lu SZ, Xu XX, Shi GG, Ye K, Zhang BR, et al. Skin Allografting Activates Anti-tumor Immunity and Suppresses Growth of Colon Cancer in Mice. *Transl Oncol.* 2018;11(4):890–9.
9. Wang Q, Meng X, Zhu L, Xu Y, Cui W, He X, Wei K, Zhu R. A polysaccharide found in *Paulownia fortunei* flowers can enhance cellular and humoral immunity in chickens. *Int J Biol Macromol.* 2019;130:213–9.
10. Pohl-Guimaraes F, Yang C, Dyson KA, Wildes TJ, Drake J, Huang J, Flores C, Sayour EJ, Mitchell DA. RNA-Modified T Cells Mediate Effective Delivery of Immunomodulatory Cytokines to Brain Tumors. *Mol Ther.* 2019;27(4):837–49.
11. Deng S, Zhang G, Kuai J, Fan P, Wang X, Zhou P, Yang D, Zheng X, Liu X, Wu Q, et al. Lentinan inhibits tumor angiogenesis via interferon gamma and in a T cell independent manner. *J Exp Clin Cancer Res.* 2018;37(1):260.
12. He J, Mu M, Luo Y, Wang H, Ma H, Guo S, Fang Q, Qian Z, Lu H, Song C. **MicroRNA–20b promotes proliferation of H22 hepatocellular carcinoma cells by targeting PTEN.** *Oncology Letters* 2019.
13. Cheng Y, Liu Y, Wei H, Sun R, Tian Z, Zheng X. Quantitation of low concentrations of polysorbates 80 in protein formulations by Coomassie brilliant blue. *Anal Biochem.* 2019;573:67–72.
14. Valenti TW, Taylor JM, Back JA, King RS, Brooks BW. Influence of drought and total phosphorus on diel pH in wadeable streams: implications for ecological risk assessment of ionizable contaminants. *Integr Environ Assess Manag.* 2011;7(4):636–47.
15. Meral I, Pala M, Akbas F, Ustunova S, Yildiz C, Demirel MH. Effects of thymoquinone on liver miRNAs and oxidative stress in Ehrlich acid mouse solid tumor model. *Biotech Histochem.* 2018;93(4):301–8.
16. Tulinska J, Adel-Patient K, Bernard H, Liskova A, Kuricova M, Ilavska S, Horvathova M, Kebis A, Rollerova E, Babincova J, et al. Humoral and cellular immune response in Wistar Han RCC rats fed

- two genetically modified maize MON810 varieties for 90 days (EU 7th Framework Programme project GRACE). *Arch Toxicol.* 2018;92(7):2385–99.
17. Zhu TT, Zhang WF, Yin YL, Liu YH, Song P, Xu J, Zhang MX, Li P. MicroRNA-140-5p targeting tumor necrosis factor-alpha prevents pulmonary arterial hypertension. *J Cell Physiol.* 2019;234(6):9535–50.
 18. Leguen I. Gills of the medaka (*Oryzias latipes*): A scanning electron microscopy study. *J Morphol.* 2018;279(1):97–108.
 19. Baghban Rahimi S, Mohebbi A, Vakilzadeh G, Biglari P, Razeghi Jahromi S, Mohebi SR, Shirian S, Gorji A, Ghaemi A. Enhancement of therapeutic DNA vaccine potency by melatonin through inhibiting VEGF expression and induction of antitumor immunity mediated by CD8 + T cells. *Arch Virol.* 2018;163(3):587–97.
 20. Tong HB, Wang Q, Lu J, Zou JM, Chang LL, Fu SY. Effect of free-range days on a local chicken breed: growth performance, carcass yield, meat quality, and lymphoid organ index. *Poult Sci.* 2014;93(8):1883–9.
 21. Yang F, Cai HH, Feng XE, Zhang YL, Ge R, Xiao BG, Li QS. 5,2'-Dibromo-2,4,5-trihydroxydiphenylmethanone, a novel immunomodulator of T lymphocytes by regulating the CD4(+) T cell subset balance via activating the mitogen-activated protein kinase pathway. *Int Immunopharmacol.* 2019;72:487–95.
 22. Zhang J, Chen Y, Chen K, Huang Y, Xu X, Chen Q, Huang C, Luo J, Lin X. IL-33 drives the antitumour effects of dendritic cells via upregulating CYLD expression in pulmonary adenocarcinoma. *Artificial Cells Nanomedicine Biotechnology.* 2019;47(1):1335–41.
 23. Wang Y, Han X, Li YD, et al. Lentinan dose dependence between immunoprophylaxis and promotion of the murine liver cancer. *Oncotarget.* 2017;8(56):95152–62.
 24. Yi-Qiang X. **Lentinan treatment of Plasmodium yoelii-infected mice induces apoptosis of regulatory T cells.** *African Journal of Biotechnology* 2012, 11(9).
 25. Terenzi A, Pirker C, Keppler BK, Berger W. Anticancer metal drugs and immunogenic cell death. *J Inorg Biochem.* 2016;165:71–9.
 26. Adeegbe DO, Nishikawa H. **Natural and Induced T Regulatory Cells in Cancer.** *Frontiers in Immunology* 2013, 4.
 27. Arthur JC, Perez-Chanona E, Mühlbauer M, Tomkovich S, Uronis JM, Fan T-J, Campbell BJ, Abujamel T, Dogan B, Rogers AB, et al. Intestinal Inflammation Targets Cancer-Inducing Activity of the Microbiota. *Science.* 2012;338(6103):120–3.
 28. Tian H, He Y, Song X, Jiang L, Luo J, Xu Y, Zhang W, Gao X, Yao W. Nitrated T helper cell epitopes enhance the immunogenicity of HER2 vaccine and induce anti-tumor immunity. *Cancer Lett.* 2018;430:79–87.
 29. Hong YP, Li ZD, Prasoon P, Zhang Q. Immunotherapy for hepatocellular carcinoma: From basic research to clinical use. *World J Hepatol.* 2015;7(7):980–92.

30. Chen L, Huang G. Antitumor Activity of Polysaccharides: An Overview. *Curr Drug Targets*. 2018;19(1):89–96.
31. Cari L, De Rosa F, Nocentini G, Riccardi C. **Context-Dependent Effect of Glucocorticoids on the Proliferation, Differentiation, and Apoptosis of Regulatory T Cells: A Review of the Empirical Evidence and Clinical Applications.** *Int J Mol Sci* 2019, 20(5).
32. Yasinska IM, Sakhnevych SS, Pavlova L, Teo Hansen Selno A, Teuscher Abeleira AM, Benlaouer O, Goncalves Silva I, Mosimann M, Varani L, Bardelli M, et al. The Tim-3-Galectin-9 Pathway and Its Regulatory Mechanisms in Human Breast Cancer. *Front Immunol*. 2019;10:1594.
33. Zhang G, Feng W, Wu J. **Down-regulation of SEPT9 inhibits glioma progression through suppressing TGF- β -induced epithelial-mesenchymal transition (EMT).** *Biomedicine & Pharmacotherapy* 2020, 125.
34. He PY, Yip WK, Jabar MF, Mohtarrudin N, Dusa NM, Seow HF. Effect of the miR-96-5p inhibitor and mimic on the migration and invasion of the SW480-7 colorectal cancer cell line. *Oncol Lett*. 2019;18(2):1949–60.
35. Zhou Q, Bauden M, Andersson R, Hu D, Marko-Varga G, Xu J, Sasor A, Dai H, Pawlowski K, Said Hilmersson K, et al. YAP1 is an independent prognostic marker in pancreatic cancer and associated with extracellular matrix remodeling. *J Transl Med*. 2020;18(1):77.
36. Shibata M, Ham K, Hoque MO. A time for YAP1: Tumorigenesis, immunosuppression and targeted therapy. *Int J Cancer*. 2018;143(9):2133–44.
37. Maurice-Dror C, Perets R, Bar-Sela G. Glucocorticoids as an adjunct to oncologic treatment in solid malignancies - Not an innocent bystander. *Crit Rev Oncol Hematol*. 2018;126:37–44.

Figures

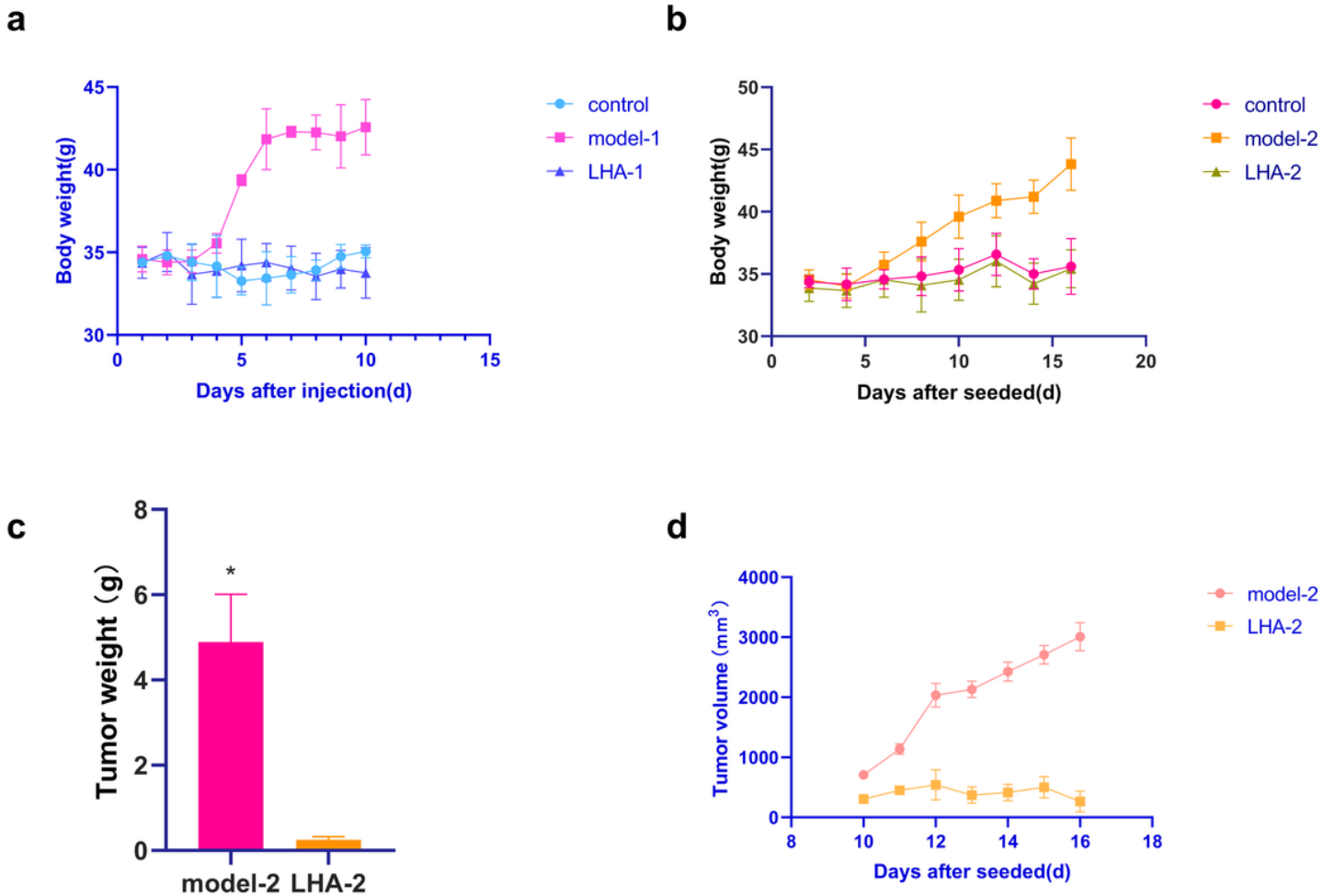


Figure 1

Effects of tumor specific antigen induced by lentinan on body weight, tumor weight and tumor volume in mice. a Changes of body weight of mice in ascites tumor group. b Changes of body weight of mice in solid tumor group. c Tumor weight of mice in solid tumor group. d Changes of tumor volume in solid tumor group.

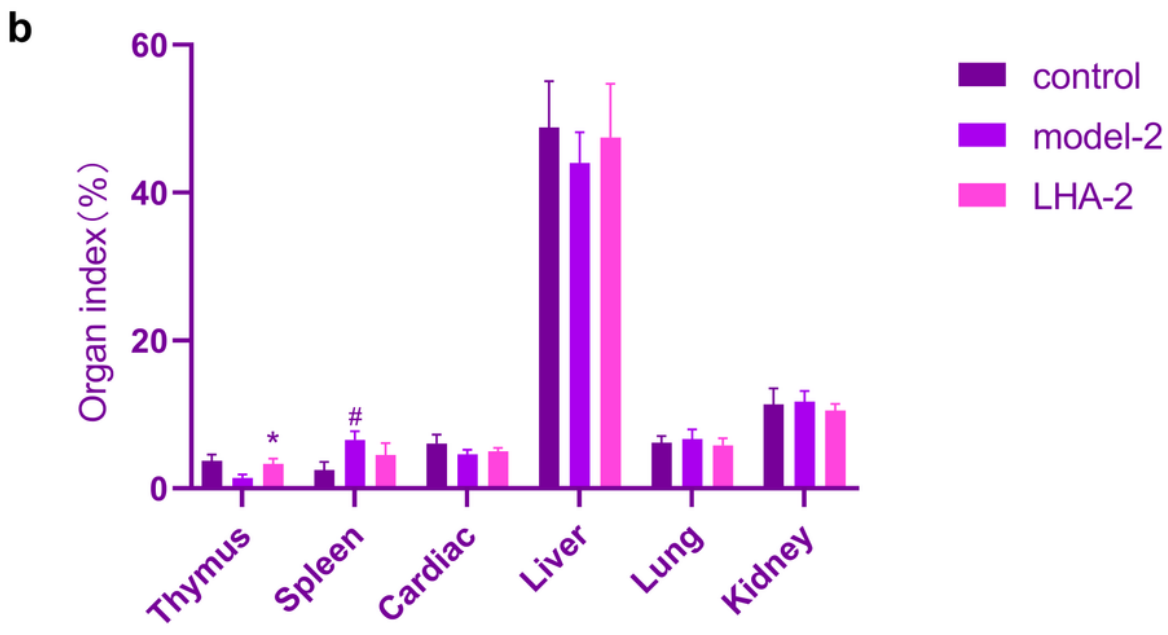
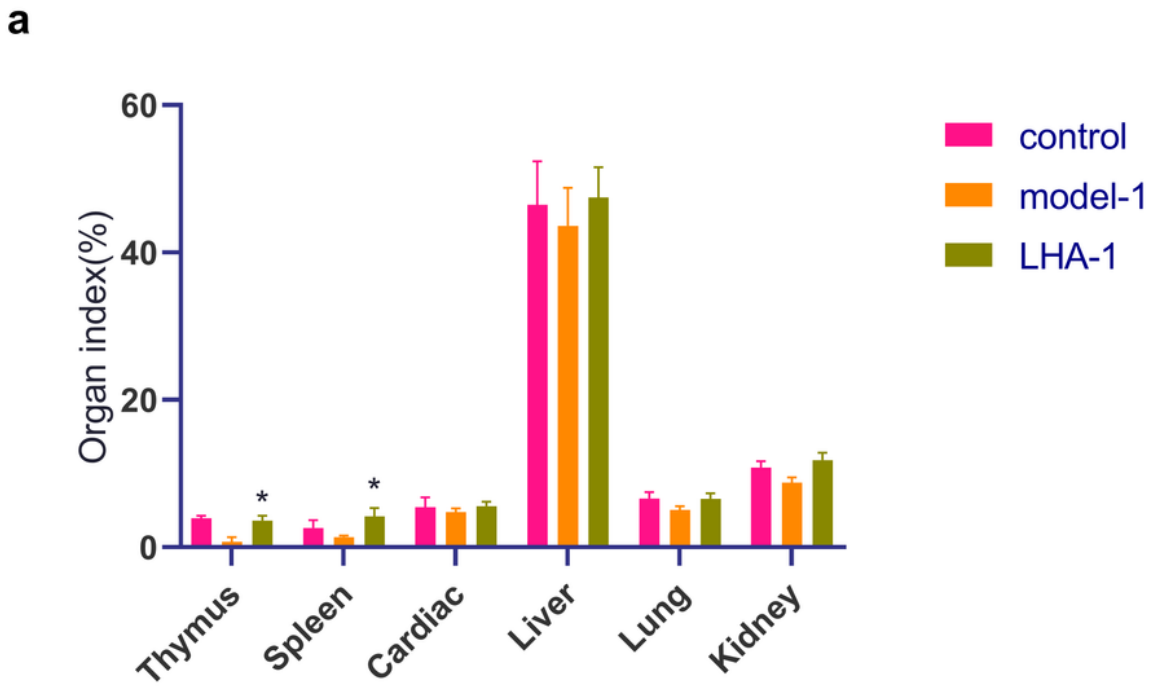


Figure 2

Comparison of organ index between LHA and model groups in solid tumor and ascites tumor mice.a Comparison of organ index between LHA-1 group and model-1 group in ascites tumor mice.b Comparison of organ index between LHA-2 group and model-2 group in solid tumor mice.

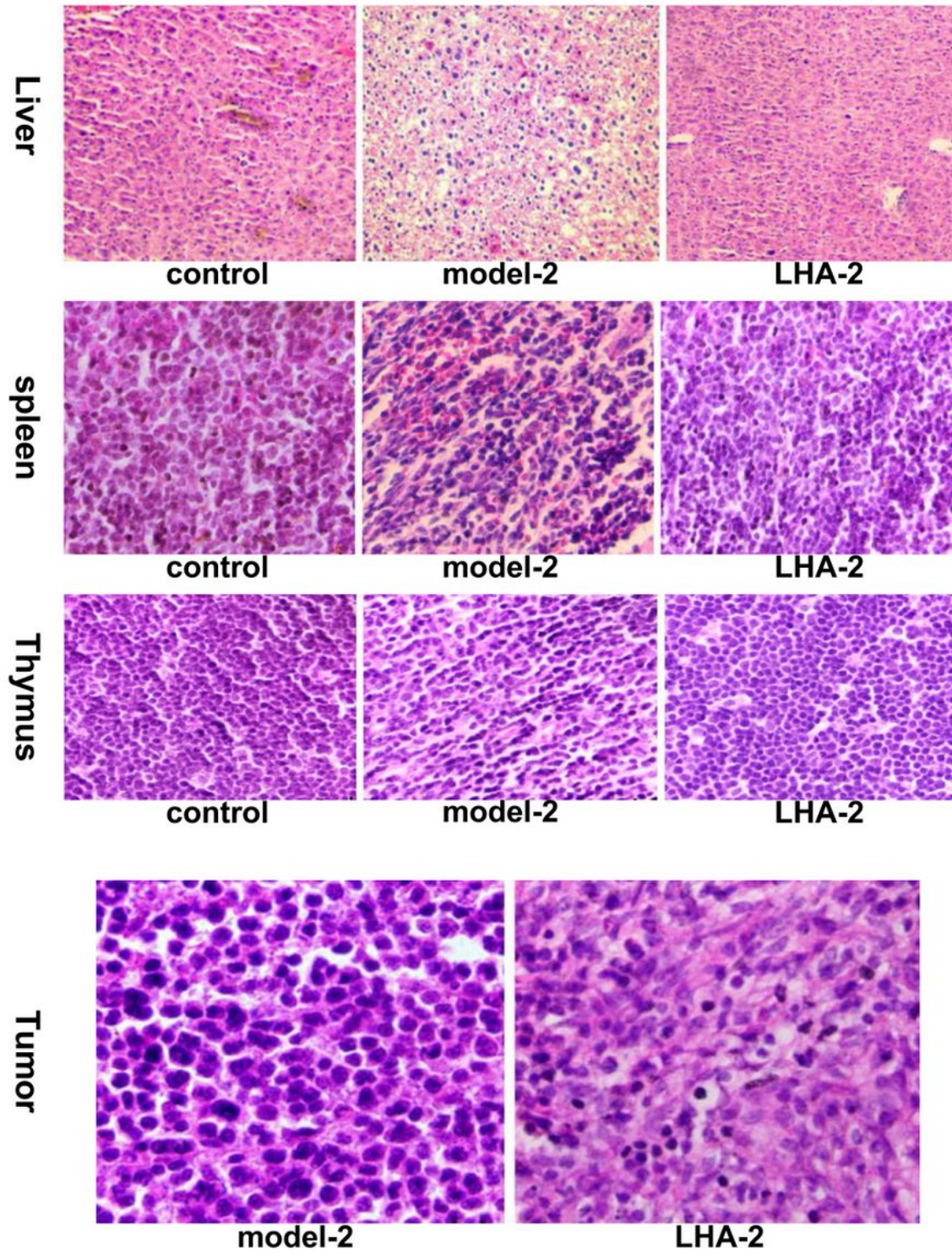
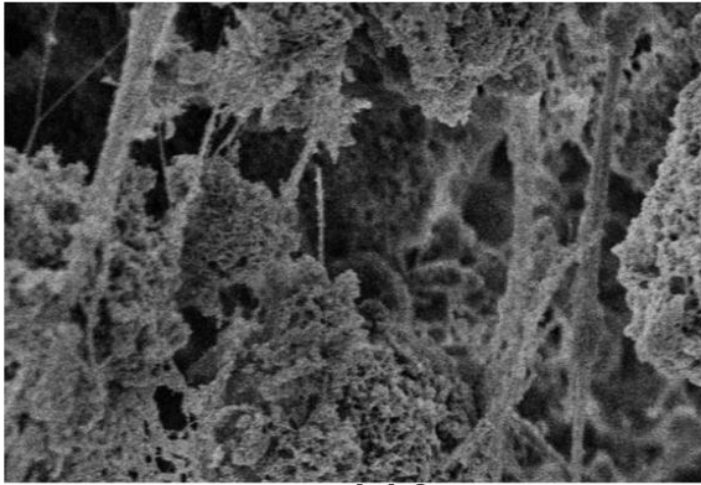
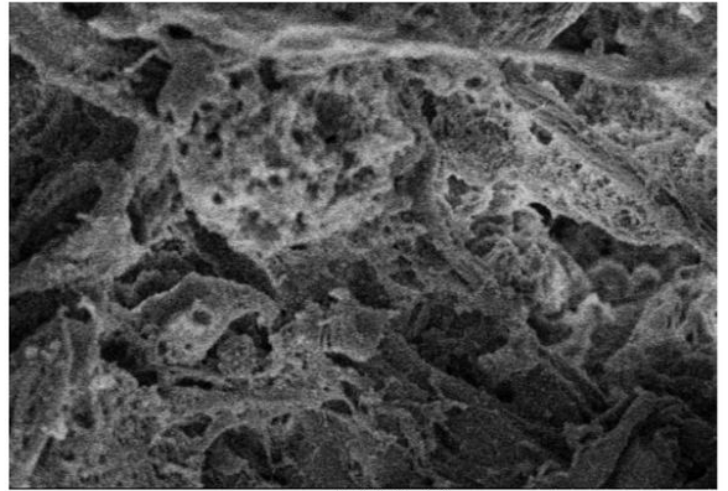


Figure 3

Analysis of tissue sections and HE staining in different groups of solid tumor mice.



model-2



LHA-2

Tumor scanning by electron microscope

Figure 4

Test results of spleen cell proliferation, CTL cell killing activity and ADCC pathway in ascites tumor mice.a Experimental results of splenocyte lymphocyte proliferation.b Detection of cytotoxicity of CTL cells in ascites tumor mice.c Detection of antibody-dependent cell-mediated cytotoxicity in ascites tumor mice.

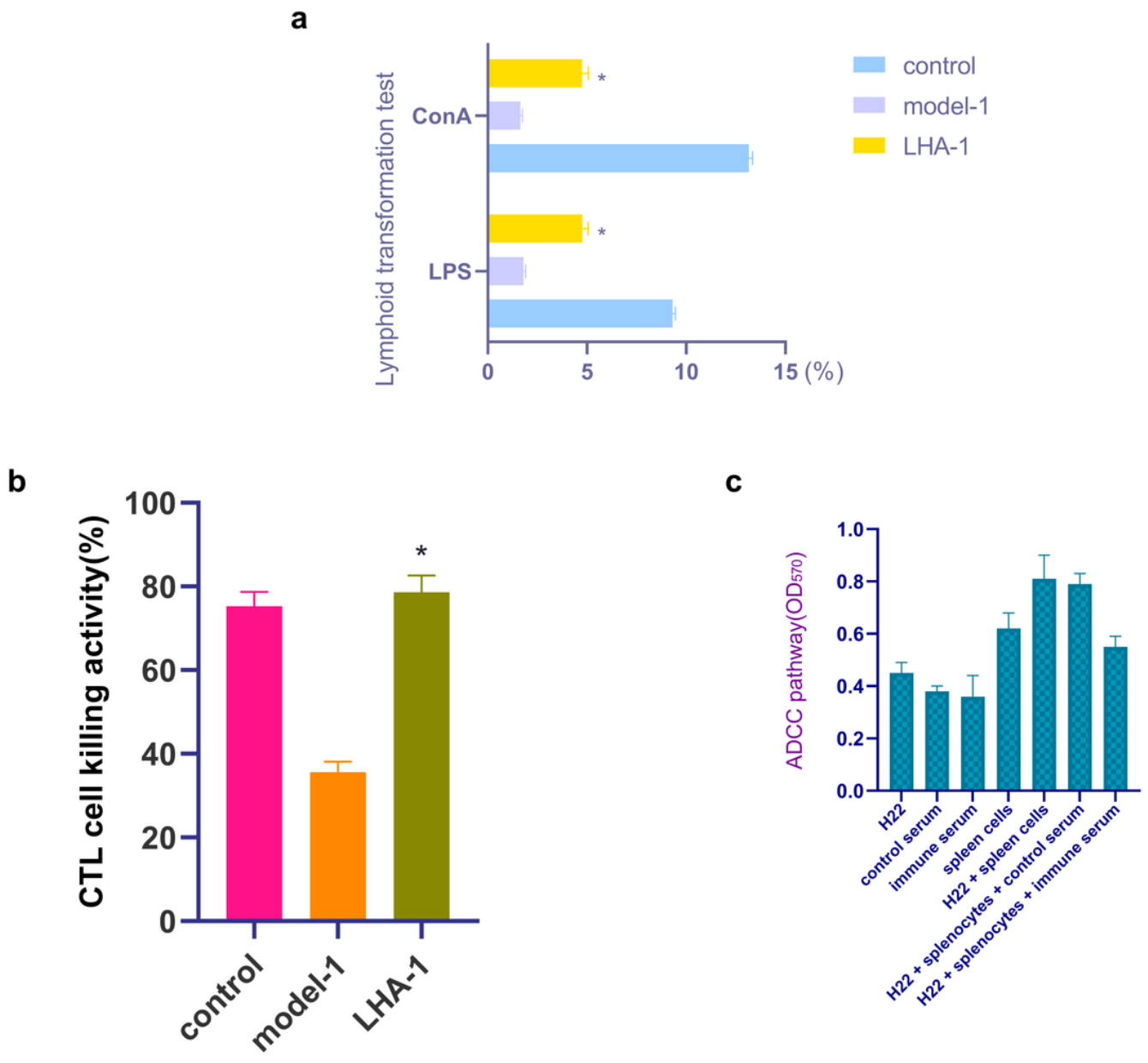


Figure 5

Test results of spleen cell proliferation, CTL cell killing activity and ADCC pathway in ascites tumor mice.a Experimental results of splenocyte lymphocyte proliferation.b Detection of cytotoxicity of CTL cells in ascites tumor mice.c Detection of antibody-dependent cell-mediated cytotoxicity in ascites tumor mice.

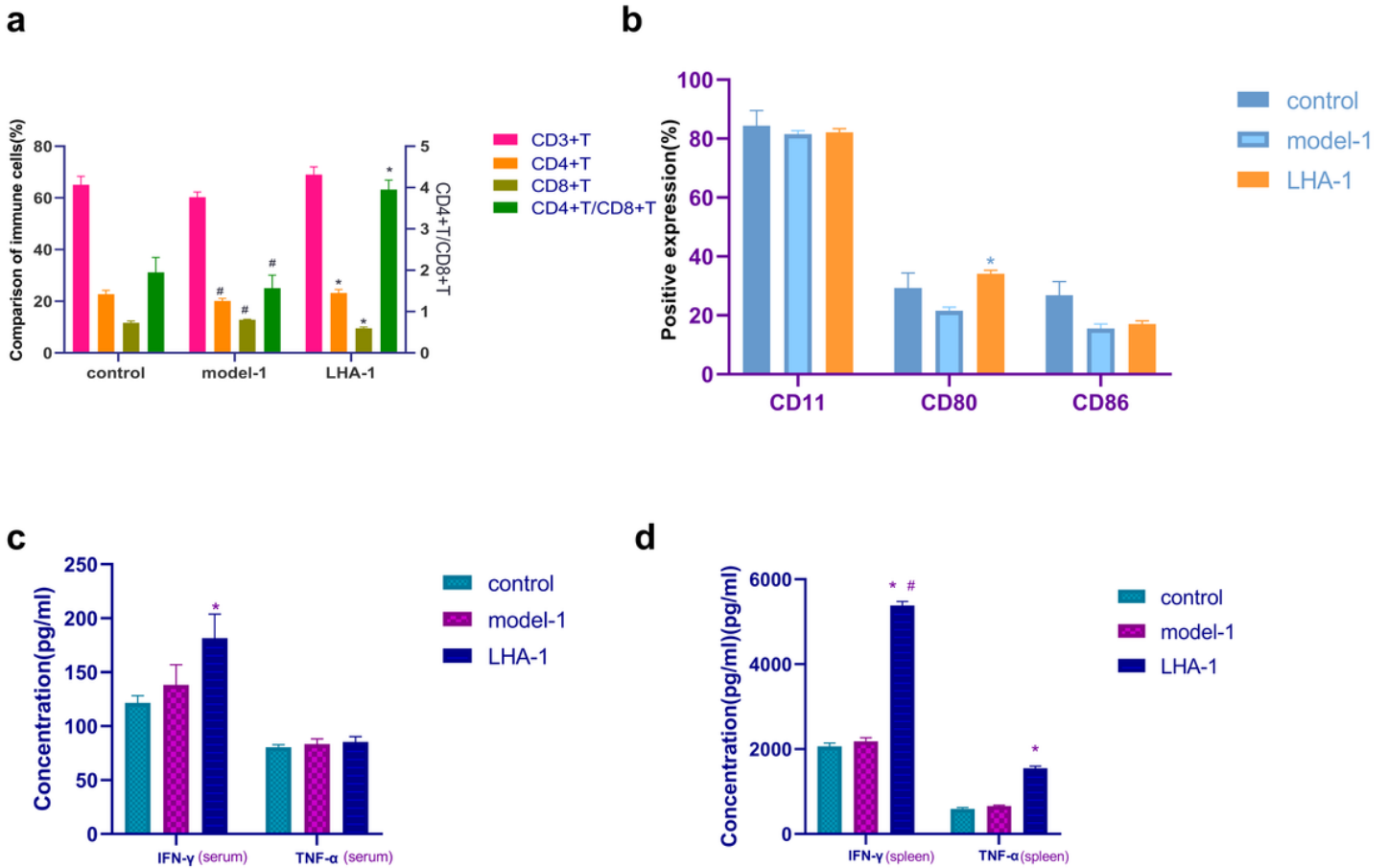


Figure 6

Detection of CD4 and CD8 phenotypes of T cells, CD80 and CD86 phenotypes of DC cells and cytokines in ascites tumor mice. a Determination of CD4 and CD8 phenotypes of T cells in mice with ascites tumor. b Determination of CD80 and CD86 phenotypes of DC cells in mice with ascites tumor. c Content of IFN-γ and TNF-α in serum of mice with ascites tumor. d Content of IFN-γ and TNF-α in splenocyte suspension of ascites tumor mice.